Australasian Physical & Engineering Sciences in Medicine (2019) 42:1099–1107
https://doi.org/10.1007/s13246-019-00809-7

SCIENTIFIC PAPER

In vivo dosimetry using MO*Skin* detector during Cobalt-60 high-dose-rate (HDR) brachytherapy of skin cancer

Z. Jamalludin[1,2,3] · W. L. Jong[2,3] · G. F. Ho[2,3] · A. B. Rosenfeld[4] · N. M. Ung[2,3]

Received: 15 April 2019 / Accepted: 16 October 2019 / Published online: 24 October 2019

Abstract
The MO*Skin*, a metal–oxide semiconductor field-effect transistor based detector, is suitable for evaluating skin dose due to its water equivalent depth (WED) of 0.07 mm. This study evaluates doses received by target area and unavoidable normal skin during a the case of skin brachytherapy. The MO*Skin* was evaluated for its feasibility as detector of choice for in vivo dosimetry during skin brachytherapy. A high-dose rate Cobalt-60 brachytherapy source was administered to the tumour located at the medial aspect of the right arm, complicated with huge lymphedema thus limiting the arm motion. The source was positioned in the middle of patients' right arm with supine, hands down position. A 5 mm lead and 5 mm bolus were sandwiched between the medial aspect of the arm and lateral chest to reduce skin dose to the chest. Two calibrated MO*Skin* detectors were placed on the target and normal skin area for five treatment sessions for in vivo dose monitoring. The mean dose to the target area ranged between 19.9 and 21.1 Gy and was higher in comparison with the calculated dose due to contribution of backscattered dose from lead. The mean measured dose at normal skin chest area was 1.6 Gy (1.3–1.9 Gy), less than 2 Gy per fraction. Total dose in EQD_2 received by chest skin was much lower than the recommended skin tolerance. The MO*Skin* detector presents a reliable real-time dose measurement. This study has confirmed the applicability of the MO*Skin* detector in monitoring skin dose during brachytherapy treatment due to its small sensitive volume and WED 0.07 mm.

Keywords Mo*Skin* · In vivo dosimetry · Skin dose · Co-60 HDR brachytherapy

Introduction

High-dose-rate (HDR) brachytherapy is a treatment of choice in some cancers due to several advantages; (a) treatment can be delivered hypo-fractionated, reducing frequent of visits which benefit the elderly and frail patients (b) rapid dose fall-off beyond the source, the most prominent characteristic of brachytherapy with increasing tumor control and sparring the surrounding tissues, and (c) dose can be delivered within a short period of time and reducing the overall treatment time. However, the delivery of high doses of HDR brachytherapy at a time necessitates real-time dose measurements to the organ at risk, including the skin during treatment.

Skin dose measurement is paramount for side effects monitoring during radiation therapy treatment. Perera et al. examined the relationship of thermoluminescent dosimeter (TLD) measured skin doses with acute and late skin and soft tissue changes in 37 patients who underwent lumpectomy HDR brachytherapy. They observed development of acute skin reaction Grade 1 or higher, telangiectasia and higher pigmentation at the points where dose exceeds 10 Gy as measured with TLD respectively at 60 months follow-up. It was concluded that dose measurement with TLD during treatment was significantly related to the afore-mentioned toxicities [1]. Thus, in vivo dosimetry (IVD) for skin dose evaluation would help in predicting the late skin toxicity related to brachytherapy treatment.

The IVD for skin dose assessment provides an independent dose verification of brachytherapy treatment planning system (TPS). Most brachytherapy TPS are currently based

✉ N. M. Ung
nm_ung@um.edu.my

1 Medical Physics Unit, University of Malaya Medical Centre, 59100 Kuala Lumpur, Malaysia

2 Department of Clinical Oncology, University of Malaya Medical Centre, 59100 Kuala Lumpur, Malaysia

3 Clinical Oncology Unit, Faculty of Medicine, University of Malaya, 50603 Kuala Lumpur, Malaysia

4 Centre for Medical Radiation Physics, University of Wollongong, Wollongong, Australia

on the TG-43 formalism, in which dose calculations are assumed to be performed in full water medium phantom, without taking into account dosimetric differences at region of different medium interface (tissue–air interface) or contribution of scattered radiation due to presence of higher density material (bone, shielding and applicator density material). At the skin–air interface, a number of studies have shown the skin doses generally were overestimated by TPS in which the real dose can be measured through IVD during treatment delivery [2–4]. IVD during HDR brachytherapy of breast carcinoma internal mammary chain using thermoluminescence detector (TLD) and metal–oxide semiconductor field-effect transistor (MOSFET) in a study by Kinhikar et al. found TPS dose overestimation by 9% [2]. In another IVD of exit skin dose study by Raffi et al., the TPS was found to overestimate the exit skin dose by an average of 16% with the use of TLD detector in HDR brachytherapy of accelerated partial breast irradiation, APBI [3]. In another dosimetry study of skin-applicator interface, the use of Freiburg flap applicator during a phantom study of skin brachytherapy treatments resulted in 6% higher TPS skin dose in comparison to dose measured with EBT3 radiochromic films [4]. The dose difference can be decreased with placement of additional bolus above the Freiburg flap applicator.

In breast brachytherapy, two common dosimeters used for IVD for skin dose assessment are TLD and MOSFET [1–3, 5]. It was reported that there was no difference in skin dose measurement using both detectors as demonstrated in study by Kinhikar et al. [2] and Choi et al. [6]. TLD detector, although found to be reliable for IVD due to water equivalent material and being small in size, possessed widely known disadvantages such as non-real time dose measurement, preparation, calibration and burdensome readout procedure. The MOSFET detectors on the other hand have the ability to produce real-time dose reading. This is important for any immediate decision on subsequent fractions dose modification and side effects prediction in situation of either under or over dose during HDR brachytherapy treatment delivery.

The MO*Skin detector* is a MOSFET-based detector with small active volume of 4.8×10^{-6} mm^3 and water equivalent depth (WED) of 0.07 mm. These special features are found to be suitable in dose measurements at the steep dose gradient region and for skin dosimetry [7, 8]. In a number of studies, MO*Skin* has proven to be reliable for IVD during tangential breast radiotherapy, electron therapy, HDR prostate and vaginal brachytherapy [6, 9–12]. Jong et al. demonstrated the clinical use of the MO*Skin* in measuring reliable skin dose during both photon tangential breast and electron boost radiotherapy treatment [9, 10].

The present study investigates the feasibility of the MO*Skin* detector to verify and measure both the target skin and unavoidable normal skin doses during HDR skin brachytherapy. Measurements were performed in a simulated phantom setup and actual skin brachytherapy procedure. The outcome of this study is expected to enhance the knowledge on MO*Skin* as a detector of choice for IVD, specifically for skin brachytherapy.

Materials and methods

Simulation and treatment planning

A 68 year-old female patient, diagnosed with recurrent breast cancer and skin involvement (Fig. 1) was decided for skin brachytherapy due to right lymphedema and inability to lift the arm for positioning in electron beam radiotherapy. Prior to computed tomography (CT) simulation, the treatment area was identified and measured for bolus and shielding lead preparation. A source holder moulded from wax with dimension of 40 mm × 40 mm with 10 mm thick was prepared. Two source holes were drilled approximately at the centre of the wax (5 mm from the surface). Both holes were 10 mm distance apart as shown in Fig. 2. CT simulation images with 2 mm scan thickness were obtained with Philips Brilliance Big Bore CT simulator (Philips Healthcare, Andover, MA). A wire was placed around the targeted skin area to aid in irradiation region identification on CT images. Figure 3 shows the treatment plan generated using the HDRplus TPS version 2.6 (Eckert and Ziegler BEBIG GmbH, Germany) to deliver 7 Gy of prescribed dose at 3 mm depth and 17 Gy to the target skin area. The treatment aim was to deliver a minimum total prescribed dose of 35 Gy at 3 mm depth in 5 fractions given within 2 weeks of treatment.

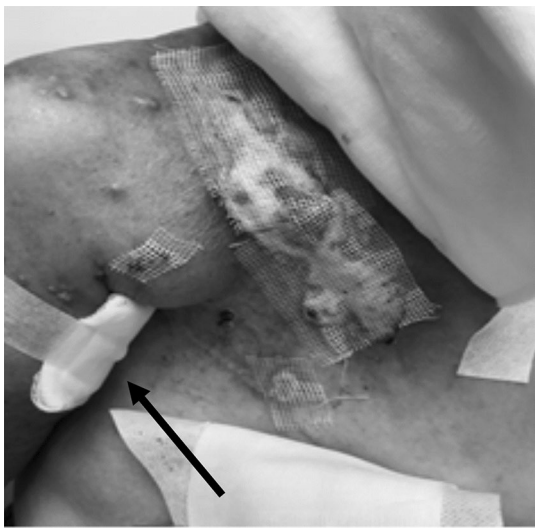

Fig. 1 Skin brachytherapy treatment area shown by the arrow on medial aspect of right arm of 68 years old female patient

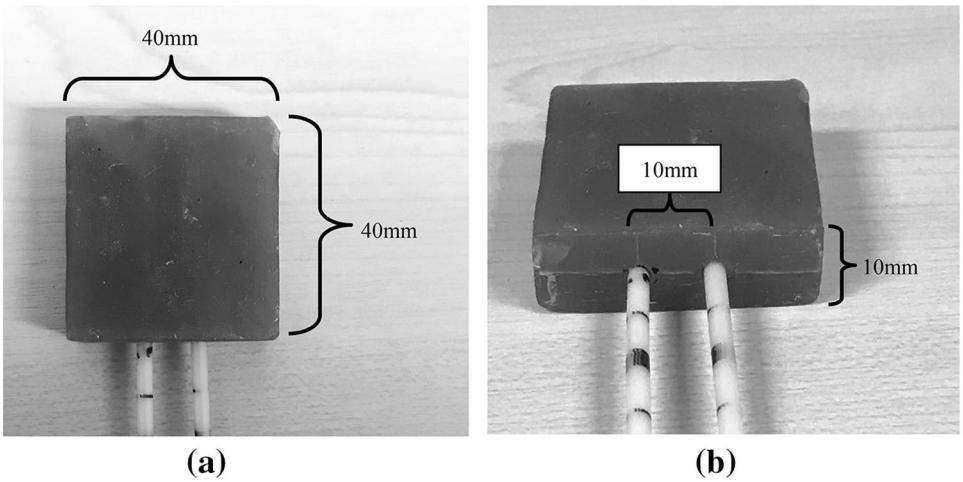

Fig. 2 **a** Dimension of wax source holder from the frontal view. **b** The wax moulded to hold the source in the centre of 10 mm thickness with 10 mm separation between two holes

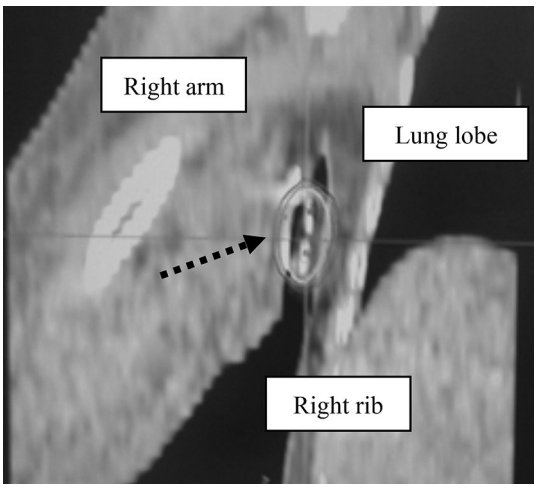

Fig. 3 Treatment plan generated by TPS showing the 7 Gy isodose lines covering the target area (shown by dash line arrow)

MO*Skin* dosimetry system

A p-channel MOSFET detector, the MO*Skin*, is a unique detector consists of a thin, flexible and reproducible polyamide film with 0.07 mm water equivalent thickness. The film acts as the build-up layer and sensor protector. The thin film thickness is equivalent to basal layer skin thickness in human and therefore, suits for skin dosimetry. By connecting to a reader, the detector is read-out in real time with a frequency of 1 Hz during treatment delivery. The MO*Skin* operates on the same principle as a conventional MOSFET detector and has been described in detail elsewhere [6–14]. The detector has been calibrated and characterized for its linearity, reproducibility, depth and angular dependence with our Cobalt-60 HDR brachytherapy source for IVD usage [15]. Prior to phantom and IVD measurement, MO*Skin* detector was calibrated in solid water phantom to deliver 1 Gy of reference dose at source–detector distance of 30 mm as described in a study from our group [15].

Phantom measurements

Based on the generated treatment plan, the close proximity of the treated lesion with right rib cage and medial lung lobe was noted, as can be seen on Fig. 3. To reduce the dose to the normal skin and right rib cage, a 5 mm lead and 5 mm bolus was placed between target skin and normal skin area during treatment. Lead served as a shielding material to reduce dose to the right rib and lung area. The additional placement of bolus increased the separation distance from the source to the normal skin area and therefore reduced the dose to the right rib and lung lobe. As the lead and bolus were not included during simulation and planning dose calculation, a phantom study was conducted to quantify; (a) potential increment of dose at the target area contributed by backscattered radiation from the placement of lead and (b) reduction of dose at the normal skin area with the placement of lead.

Three different lead–bolus setup arrangements were simulated as shown in Fig. 4 to investigate the impact of these arrangements on doses to the target as well as the normal skin. Measurements were conducted in polymethyl methacrylate (PMMA) phantom with a dimension of $300 \times 300\,\text{mm}^2$. A slab of 100 mm thick PMMA was placed on top of the source wax holder, representing thickness of target area while the last layer of 100 mm thick PMMA slab represented the thickness of normal tissue. Two MO*Skin* detectors were placed at each target and normal PMMA phantom for dose measurement. Then, three different lead–bolus configurations in between these target and normal slab were arranged as follows; setup (a) two layers of 5 mm thick bolus below the source, denoted as setup 'SBB', setup (b) a 5 mm lead below the source, followed by a layer of 5 mm bolus, hereafter in the text 'SLB' setup and, setup (c) a layer of 5 mm bolus below the source, followed by

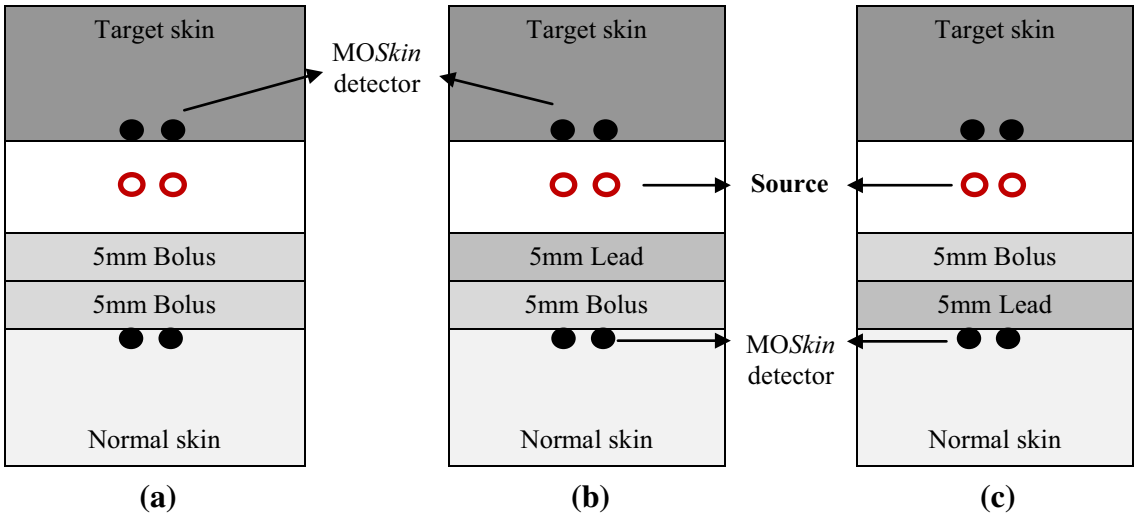

Fig. 4 Three different phantom setup arrangement of source–lead–bolus; **a** source and two layers of bolus sandwiched between target and normal skin, denoted as SBB, **b** arrangement of source, followed by lead and bolus denoted as SLB, and **c** arrangement of source, followed by bolus and lead, denoted as SBL. Two MO*Skin* detectors located at each the target and normal skin area. Noted that distance from source to detectors at the target skin and normal skin for all setup remain the same of 5 mm and 15 mm respectively

5 mm lead, referred as 'SBL' setup. The distances from the source to MO*Skin* detector placed at the target and normal skin area in all setups were 5 mm and 15 mm respectively. These distances represented the actual source–detector distance during treatment. Phantom was scanned under CT simulator based on patient simulation procedure and parameters as described in "Simulation and treatment planning" section. Using the same patient's generated treatment plan by the TPS from "Simulation and treatment planning" section, doses to the MO*Skin* detectors on the phantom were calculated. With Cobalt-60 source activity of 49.82 GBq, the total irradiation time planned for the treatment was 329.90 s to deliver 7 Gy dose at 3 mm depth and 17 Gy skin dose of the target area. Measurements in each phantom setup were repeated three times to obtain the mean readings. The TPS calculated doses were compared with MO*Skin* measured dose for all the three different phantom setups.

In vivo measurements

An Eckert and Ziegler BEBIG MultiSource® HDR remote after-loader brachytherapy treatment unit model 1322–0012 (Eckert and Ziegler, Germany) with Cobalt-60 source (average energy of 1.25 MeV) was used for the treatment. The Co-60, model Co0.A86 is composed of a 3.5 mm long and 0.5 mm diameter central cylindrical active core made of metallic cobalt, containing Co-60 source. With its' initial activity of 68.05 GBq calibrated on 11th February 2016, the source strength was verified locally using a PTW (Physikalisch-Technishe Werkstatten GmbH, Freiburg, Germany) well-type ionization chamber and within 2% ± agreement with vendor's stated source strength. Written informed consent was obtained from the patient prior to measurement. Similar to phantom setup, two MO*Skin* detectors were placed directly on skin target area and another two detectors on opposite normal tissues, perpendicular to the target area with detectors active volume facing the source as shown in Fig. 5. Based on recommendation from other studies, a period of 1 min was given to the detectors to reach thermal equilibrium before treatment irradiation [6, 10, 15, 16]. The MO*Skin* detectors response were then converted into absorbed dose by incorporating the distance correction factors for Cobalt-60 source application as determined in our previous study [15].

Results

Figure 6 shows the comparison of mean MO*Skin* measured doses from the three source–lead–bolus arrangement setup in the phantom study with calculated doses from TPS. It was noted the SLB setup produced higher doses to the target skin area while setup SBL resulted in lower doses to the normal skin area. There were small percentage dose differences between mean measured doses from SBB with calculated TPS doses as can be seen from Table 1 with an average of 2.9% and − 2.2% for dose differences at target and normal skin area respectively. The mean MO*Skin* measured doses at the target area for both SLB and SBL setups were found to be higher. However, the SLB setup resulted in much higher mean doses to the target area with an average of 24% in comparison to only 5% from SBL setup as can be seen in Table 1.

Fig. 5 Treatment setup showing the application of source–lead–bolus arrangement with source transfer tube in place

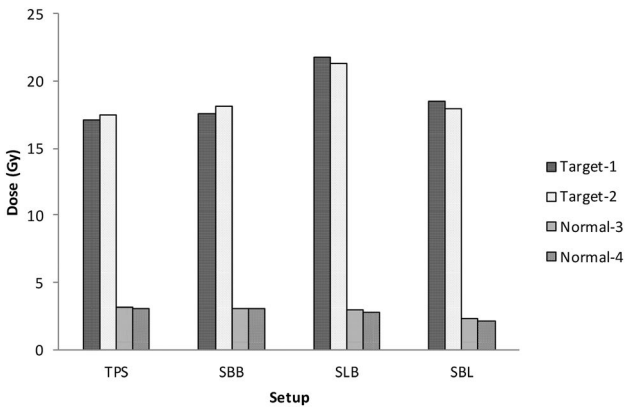

Fig. 6 MO*Skin* measured dose at both tumor and normal tissue regions for three different source–lead–bolus arrangement setups. Dose calculated from TPS regarded as reference for dose comparison

On contrary, the SBL setup was found to reduce more doses to the normal tissue in comparison with the SLB setup with an average of 29% and 7% respectively.

Table 2 summarizes the in vivo measured skin doses at both the target and normal skin area for all treatment fractions with the application of setup SLB. The mean dose to the skin target area for each fraction was 20.5 Gy with 0.03% coefficient of variations between fractions. When comparing the mean target dose of single fraction to the planned dose from TPS of 17 Gy, the backscattered radiations due to the presence of lead contributed to additional 20.7% dose to the target area. This was found to be comparable to the lead dose contribution measured in the phantom study. The mean dose to the normal skin area in single fraction was 1.6 Gy with coefficient of variation of 0.17% between fractions. These measured doses during treatment were found to be reduced by 55%, in comparison to the measured normal skin dose from the phantom study. By comparing the measured normal skin dose with TPS calculated dose without lead and bolus placement, the dose was reduced by approximately 80%. The mean normal skin dose for each fraction was below 2.0 Gy. The mean total physical dose at both the target and normal skin was 102.6 Gy and 7.8 Gy respectively. Using α/β ratio of 10 and 2 for target and normal skin, the biologically equivalent doses for 2-Gy per fractions (EQD_2) was calculated to be 260.9 Gy and 6.9 Gy accordingly [17]. The differences in target and normal skin dose measurement between fractions may be due to differences in applied pressure from the patient during irradiation which may cause the detectors to be further away or nearer to the brachytherapy source during treatment. Although proper marking of wax holder, bolus, lead and detector location was performed which was expected to produce a reliable and reproducible setup, inconsistencies in the applied pressure was beyond the operator's and patient's control.

Discussion

This study quantifies the percentage of dose contribution to the skin target area and dose reduction at normal skin with the lead placement from two different lead–bolus arrangements measured in phantom setup. Both SLB and SBL

Table 1 Mean measured dose in phantom for three different source–lead–bolus setup arrangements

Area	TPS (Gy)	(a) SBB (Gy)	% Difference	(b) SLB (Gy)	% Difference	(c) SBL (Gy)	% Difference
Target-1	17.17	17.56 ± 0.06	2.3	21.74 ± 0.10	26.6	18.54 ± 0.05	8.0
Target-2	17.50	18.11 ± 0.19	3.5	21.32 ± 0.29	21.8	17.96 ± 0.12	2.6
Normal-3	3.17	3.10 ± 0.01	− 2.1	3.01 ± 0.01	− 4.9	2.33 ± 0.01	− 26.4
Normal-4	3.10	3.03 ± 0.01	− 2.3	2.79 ± 0.13	− 10.0	2.10 ± 0.02	− 32.3

Target-1 and 2 refer to the MO*Skin* detectors located at the target skin phantom while Normal-3 and 4 refer to detectors at normal skin phantom

Table 2 In vivo dosimetry measured doses using MO*Skin* detectors on skin target and normal skin area for each fraction

Fractions	Target skin 1 (Gy)	Target skin 2 (Gy)	Mean target skin (Gy)	Normal skin 3 (Gy)	Normal skin 4 (Gy)	Mean normal skin (Gy)
1	20.27	21.61	20.94	1.25	1.36	1.31
2	20.13	22.05	21.09	1.99	1.97	1.98
3	19.91	20.07	19.99	1.12	1.78	1.45
4	19.80	20.01	19.91	1.31	1.58	1.44
5	20.66	21.49	20.66	1.59	1.60	1.60
	Total physical dose (Gy)		~102.6	Total physical dose (Gy)		~7.8
	Total EQD_2 dose (Gy)		~260.9	Total EQD_2 dose (Gy)		~6.9

setups resulted in different percentages of dose enhancement to the target area and dose reduction to normal skin area. A higher dose enhancement at target area was resulted from the SLB setup while larger dose reduction to normal skin can be achieved with the SBL setup. In SLB setup, the 5 mm distance from lead to brachytherapy source was much shorter in comparison to 10 mm lead–source distance in the SBL setup. With shorter lead–source distance, the lead in the SLB setup was located in the high dose gradient region. Hence, the intensity of photons reaching the lead was much higher, producing higher amount of backscattered radiation towards the target area and thus increasing dose to the target area. Following the inverse square law, at lead–source distance of 10 mm, photon intensities reaching lead in SBL setup were lower, resulting in less backscattered radiation and doses to the target area. Due to favorable dosimetry at the target area, setup SLB was chosen to be applied for treatment with aim to increase dose at the skin target area while having optimal dose reduction to the normal tissue. This lead–bolus arrangement also indirectly helped to avoid direct contact of patients' normal skin with lead which may bring discomfort to the patient.

The placement of lead with aim to shield and reduce dose to unavoidable normal tissues or organ at risk has caused dose enhancement at both backscattered and forward regions at which the TPS is unable to estimate accurately [18–22]. Interface dosimetry needs to be performed with detectors having small thickness which are able to measure dose exactly at and beyond the interface for accurate dose estimation. Detectors such as EBT gafchromic film and MO*Skin* had been shown to be suitable for such measurements [21, 22]. In the measurement of percentage depth-dose and beam profiles at water–steel phantom interface, both the EBT2 and MO*Skin* detectors were able to measure dose enhancement and reduction at and beyond the interface respectively and were in good agreement with Monte Carlo calculations under 6 MV photon beam [21]. Since dose enhancement is unavoidable with lead placement, several factors such as choices of lead–bolus thickness and arrangement need to be considered in order to reduce the percentage of dose enhancement to both target and normal skin regions.

Factors contributing to dose enhancement at both regions has been studied by Li et al. in a water phantom being irradiated by various high-energy photon for range of lead thickness. The results indicated that dose enhancement near interface was primarily due to contributions of secondary electrons [18]. However, the percentage of dose enhancement within depth range for both directions were found to be different in a study by Lliso et al. Dose enhancement at the backscattered region increased up to 200% within 0.5 mm depth range as compared to 130% within 1.0 mm depth in forward region [19]. Due to the existence of dose enhancement before and behind the lead, two layers of 0.5 mm and 1.0 mm bolus were suggested to be placed accordingly to attenuate the scattered radiation. However, in our study, only one layer of bolus was applied in both phantom measurement and treatment delivery. Limited by the patient comfort, maximum separation of only 20 mm distance between right arm and right lateral chest can be achieved as the patient was unable to lift the arm further. This allowed us to place the wax holder and 5 mm lead with only one layer of 5 mm bolus. Consequently, the absence of bolus layer before lead in our study which gives higher backscattered dose is a prominent advantage to increase dose to the target area.

A previous study of the use of 3 mm lead plate thickness in a phantom irradiated with Cobalt-60 source resulted in lower mean photon energy in backscattered direction in comparison to the placement of 6 mm and 10 mm thick lead plate [20]. In the present study, a 5 mm thick lead plate was used as we were unable to produce a 3 mm lead plate. This produced slightly higher mean photon energy of the backscattered radiation compared to 3 mm lead application [20] and hence, resulted in higher dose contribution from the backscattered radiation to the target area. However, the number of photon transmitted through lead decreased with lead thickness which is paramount for dose reduction to normal tissue. As such, the choice of lead plate thickness should be balanced between the aim to increase dose to the target area

and reducing dose to the normal tissue region. Regardless of lead plate thicknesses, the backscattered dose found to reach up to 3 mm depth with Co-60 source as opposed to only 1 mm depth with Iridium-192 source [20]. This effect will be more prevalent and improved with the application of Iridium-192 as brachytherapy source.

The uncertainties with utilization of MO*Skin* as IVD detector in this study were estimated as shown in Table 3. Uncertainties related to the application of MO*Skin* for IVD in prostate and vaginal brachytherapy using Ir-192 source were estimated by Carrara et al., in two separated studies [11, 12]. With MO*Skin* uncertainties under Co-60 brachytherapy source have been estimated in water equivalent medium by Jamalludin et al., uncertainties from the above-mentioned studies were included in Table 3. For uncertainties related to dose calculation, Table 4 outlined the estimated measurements uncertainties with values reported in this table were taken mainly from Kirisits et al. which outlined the uncertainty in clinical brachytherapy. The total uncertainty budget with regards to MO*Skin* dose measurement is 5.2% while dose point calculation uncertainty with TPS is 8.4%.

To the best of our knowledge, the application of MO*Skin* as detector for in vivo skin dose measurements during brachytherapy treatment has not been explored by other studies, specifically for Cobalt-60 brachytherapy source. MO*Skin* dosimeter has been used in assessment of skin–air interface effect on skin dose during HDR brachytherapy APBI [23]. As the accuracy of dose at the interface calculated by the available brachytherapy TPS is known to be poor, a phantom study was conducted. Measurement performed with MO*Skin* on a surface of the gel breast phantom, mimicking the clinical treatment demonstrated lower dose when compared to planned doses [23]. Based on this, an on-going study on conducting the real-time skin dose measurement with MO*Skin* detector during APBI treatment is being developed.

Table 4 Estimated measurement uncertainties from treatment planning system

Sources of measurement uncertainties	Estimated uncertainty (%) (k = 1)
(a) Intrinsic dose point calculation	
• Treatment planning dose calculation	± 3.0[a]
• Medium dosimetric correction	± 3.0[a]
• Air kerma strength (S_k) source determination	± 2.0[a]
(b) Image-related dose point calculation	
• Dose delivery including registration of applicator geometry to anatomy	± 7.0[a]
Total measurement uncertainty	± 8.4

[a]According to Kirisits et al. [29]

MO*Skin* previously has been used to assess skin dose during external beam radiotherapy treatment. In a phantom study on assessment of skin dose owing to the use of cast material for breast immobilization during breast radiotherapy, a significant higher skin dose was measured using the MO*Skin* detector [24]. Choi et al. measured a stable skin dose reading over every measurements points with maximum percentage dose difference of 8.2% and 4.5% with TLD conducted in phantom under clinical conditions of total skin electron therapy treatment [6]. In an in vivo skin dose study during breast radiotherapy without bolus application, the MO*Skin* reading was found to be lower than EBT2 film [9]. Due to slight difference in WED of gafchromic EBT film detector, MO*Skin* measured skin doses were lower than film measured doses as demonstrated in a number of studies [6, 9, 10, 25]. As the ICRP recommended depth of skin dose measurement is 0.07 mm, dose measurement using MO*Skin*

Table 3 Estimated detector uncertainties with MO*Skin* as detector

Sources of detector uncertainties	Estimated uncertainty (%) (k = 1)
(a) MO*Skin* calibration	
• Air kerma strength (S_k) source determination	± 2.0[a]
• Further dose calibration (phantom assembly, source to MO*Skin* distance, AAPM-TG43 parameters for dose calculation)	± 1.0[b]
(b) MO*Skin* intrinsic	
• Temperature dependence, reproducibility and MO*Skin* readout system resolution	± 1.5[b]
• Intra-fraction MO*Skin* degradation	± 1.5[b]
• Energy (distance) dependence	± 1.8[c]
• Polar angular dependence	± 3.2[c]
• Azimuth angular dependence	± 1.9[c]
Total measurement uncertainty	± 5.2

[a]According to Kirisits et al. [29]

[b]According to Carrara et al. [12]

[c]According to Jamalludin et al. [30]

detector can be considered as more reliable in measuring dose at the skin compared to EBT film in these studies.

When MO*Skin* detector was placed at skin for skin dose IVD, the thickest part of detector is expected to increase the skin dose at respective area underneath the MO*Skin* detector during high energy photon radiotherapy. Using the solid water slab phantom, this effect has been studied by Alnawaf et al. for both 6 MV and 10 MV photon beam using for number of file sizes. Regardless of the field size dimensions, this study found a $14 \pm 1\%$ and $9.5 \pm 0.5\%$ dose increment measured at the region under MO*Skin* detector active volume for 6 MV and 10 MV photon beam respectively. This impact however was found to be minimal when comparing to 32% and 26% increase in dose when measured using TLD detector. This study concluded the dose increment did not affect the reliability of the MO*Skin* detector for skin dose measurement [26].

The National Surgical Adjuvant Breast and Bowel Project B-39/Radiation Therapy Oncology Group 04–13 (NSABP B39/RTOG 04–13) recommended the maximal skin dose of an acceptable APBI brachytherapy planning to be $\leq 145\%$ prescribed dose (38.5 Gy in 10 fractions) to reduce the skin toxicity events [27]. Further reduction of maximum skin dose tolerance was suggested by Cuttino et al. as maximal skin dose of > 4.05 Gy per fraction resulted in significant association with incidence of telangiectasis in a large patients cohort (96 patients) with prolonged follow-up (median of 48 months) [27]. In a more recent study, an updated maximal skin dose tolerance has been proposed by Vargo et al. from the findings in 157 patients with median > 5 years follow up. This study found a stronger predictor for telangiectasis development with skin dose $> 100\%$ (34 Gy) than prior studies recommended constraint [28]. The normal skin dose measured for each fraction in our study nevertheless, was found to be less than 2 Gy for each fraction. As the total EQD_2 for normal skin dose was calculated to be less than 20 Gy, the measured normal skin doses for this patient was below the above-mentioned recommended skin dose level tolerance for late toxicity occurrence. In addition, the value was also below the tolerance dose level for skin erythema [9]. The MO*Skin* measured dose at both target and normal skin region which is useful to monitor the development of any skin toxicity for proper clinical management of skin reactions.

Although data relating chest wall/rib doses during brachytherapy with toxicities are scarce, excessive chest wall/rib doses potentially can cause rib fractures and/or chest wall discomfort in some patients [27]. Thereby, dosimetric goals of limiting the chest wall/ribs dose below ≤ 50 Gy with intention to reduce toxicity to ribs were stated in study by Cuttini et al. In our study, the dose to the right rib determined from TPS was 1.6 Gy/fraction. Translating this value into the dose measured during treatment with lead and bolus in place, the total dose received by the right ribs calculated to be approximately $<$ than 2 Gy, which is well below the maximal ribs dose tolerance from Cuttini et al.

Conclusion

The dose assessment for three different source–lead plate–bolus arrangements provides useful information on the percentage dose increment and reduction to the target and normal skin area. Owing to patient comfort and condition, the best arrangement was decided without compromising the target dose coverage and dose reduction to the normal skin area. The MO*Skin* detector presents a reliable real-time dose measurement and has proven to be effective for IVD of skin dose measurement in phantom and in vivo brachytherapy. This study has verified the MO*Skin* applicability in monitoring skin dose during brachytherapy treatment due to its small sensitive volume and thickness.

Acknowledgements The authors would like to thank all the radiographers, technician, medical officers and staff nurse in Department of Clinical Oncology, University of Malaya Medical Centre for the assistance in this work. This study was supported by Postgraduate Research Grant (PPP) Project No. PG211-2015B, Faculty of Medicine, University of Malaya, Malaysia.

Compliance with ethical standards

Ethical approval All procedures performed in studies involving human participants were in accordance with the Ethical Standards of the University of Malaya Medical Centre Research Committee (MECID No. 2017123–4840) and with the 1964 Helsinki Declaration and its later amendments or comparable ethical standards.

References

1. Perera F, Chisela F, Stitt L et al (2005) TLD skin dose measurements and acute and late effects after lumpectomy and high-dose-rate brachytherapy only for early breast cancer. Int J Radiat Oncol Biol Phys 62:1283–1290. https://doi.org/10.1016/j.ijrobp.2005.01.007
2. Kinhikar RA, Sharma PK, Tambe CM et al (2006) Clinical application of a OneDose^{TM} MOSFET for skin dose measurements during internal mammary chain irradiation with high dose rate brachytherapy in carcinoma of the breast. Phys Med Biol. https://doi.org/10.1088/0031-9155/51/14/N01
3. Raffi JA, Davis SD, Hammer CG et al (2010) Determination of exit skin dose for ^{192}Ir intracavitary accelerated partial breast irradiation with thermoluminescent dosimeters. Med Phys 37:2693–2702. https://doi.org/10.1118/1.3429089
4. Aldelaijan S, Bekerat H, Buzurovic I et al (2017) Dose comparison between TG-43–based calculations and radiochromic film measurements of the Freiburg flap applicator used for high-dose-rate brachytherapy treatments of skin lesions. Brachytherapy 16:1065–1072. https://doi.org/10.1016/j.brachy.2017.06.011
5. Selvaraj RN, Bhatnagar A, Beriwal S et al (2007) Breast skin doses from brachytherapy using MammoSite® HDR, intensity

modulated radiation therapy, and tangential fields techniques. Technol Cancer Res Treat 6:17–22. https://doi.org/10.1177/153303460700600103
6. Choi JH, Cutajar D, Metcalfe P, Downes S (2018) Application of MOSkin detector for in vivo dosimetry on total skin electron therapy (TSET). Biomed Phys Eng Express. https://doi.org/10.1088/2057-1976/aaac61
7. Hardcastle N, Cutajar DL, Metcalfe PE et al (2010) In vivo real-time rectal wall dosimetry for prostate radiotherapy. Phys Med Biol 55:3859–3871. https://doi.org/10.1088/0031-9155/55/13/019
8. Tenconi C, Carrara M, Borroni M et al (2014) TRUS-probe integrated MOSkin detectors for rectal wall in vivo dosimetry in HDR brachytherapy: in phantom feasibility study. Radiat Meas 71:379–383. https://doi.org/10.1016/j.radmeas.2014.05.010
9. Jong WL, Ung NM, Wong JHD et al (2016) In vivo skin dose measurement using MOSkin detectors in tangential breast radiotherapy. Phys Med 32:1466–1474. https://doi.org/10.1016/j.ejmp.2016.10.022
10. Jong WL, Ung NM, Tiong AHL et al (2018) Characterisation of a MOSFET-based detector for dose measurement under megavoltage electron beam radiotherapy. Radiat Phys Chem 144:76–84. https://doi.org/10.1016/j.radphyschem.2017.11.021
11. Carrara M, Tenconi C, Rossi G et al (2016) In vivo rectal wall measurements during HDR prostate brachytherapy with MOSkin dosimeters integrated on a trans-rectal US probe: comparison with planned and reconstructed doses. Radiother Oncol 118:148–153. https://doi.org/10.1016/j.radonc.2015.12.022
12. Carrara M, Romanyukha A, Tenconi C et al (2017) Clinical application of MOSkin dosimeters to rectal wall in vivo dosimetry in gynecological HDR brachytherapy. Phys Med 41:5–12. https://doi.org/10.1016/j.ejmp.2017.05.003
13. Ian K, Andrew H, Michael L et al (2008) Measurement of rectal dose during HDR brachytherapy using the new MOSkin dosimeter. J Nucl Sci Technol 45:481–484. https://doi.org/10.1080/00223131.2008.10875895
14. Qi Z, Deng X, Huang S et al (2007) Verification of the plan dosimetry for high dose rate brachytherapy using metal–oxide-semiconductor field effect transistor detectors. Int J Med Phys Res Pract 34:2007–2013. https://doi.org/10.1118/1.2736288
15. Jamalludin Z, Jong WL, Abdul Malik R et al (2019) Characterization of MOSkin detector for in vivo dose verification during cobalt-60 high dose-rate intracavitary brachytherapy. Phys Med 58:1–7. https://doi.org/10.1016/j.ejmp.2019.01.010
16. Jong WL, Wong JHD, Ung NM et al (2014) Characterization of MOSkin detector for in vivo skin dose measurement during megavoltage radiotherapy. J Appl Clin Med Phys 15:120–132. https://doi.org/10.1120/jacmp.v15i5.4869
17. Nag S, Gupta N (2000) A simple method of obtaining equivalent doses for use in HDR brachytherapy. Int J Radiat Oncol Biol Phys 46:507–513. https://doi.org/10.1016/S0360-3016(99)00330-2
18. Li XA, Chu JCH, Chen W, Zusag T (1999) Dose enhancement by a thin foil of high-Z material: a Monte Carlo study. Med Phys 26:1245–1251. https://doi.org/10.1118/1.598619
19. Lliso F, Granero D, Perez-Calatayud J et al (2011) Dosimetric evaluation of internal shielding in a high dose rate skin applicator. J Contemp Brachytherapy 3:32–35. https://doi.org/10.5114/jcb.2011.21041
20. Candela-Juan C, Granero D, Vijande J et al (2014) Dosimetric perturbations of a lead shield for surface and interstitial high-dose-rate brachytherapy. J Radiol Prot 34:297–311. https://doi.org/10.1088/0952-4746/34/2/297
21. Alhakeem EA, AlShaikh S, Rosenfeld AB, Zavgorodni SF (2015) Comparative evaluation of modern dosimetry techniques near low- and high-density heterogeneities. J Appl Clin Med Phys 16:142–158. https://doi.org/10.1120/jacmp.v16i5.5589
22. Rosenfeld AB, Wong JHD, Jong WL et al (2017) Dosimetric evaluation near lung and soft tissue interface region during respiratory-gated and non-gated radiotherapy: a moving phantom study. Phys Med 42:39–46. https://doi.org/10.1016/j.ejmp.2017.08.011
23. Carrara M, Cutajar D, Alnaghy S et al (2018) Semiconductor real-time quality assurance dosimetry in brachytherapy. Brachytherapy 17:133–145. https://doi.org/10.1016/j.brachy.2017.08.013
24. Metcalfe P, Kelly A, Hardcastle N et al (2010) Surface dosimetry for breast radiotherapy using MOSkins to measure the influence of immobilization cast material. Int J Radiat Oncol Biol Phys 78:S762–S763. https://doi.org/10.1016/j.ijrobp.2010.07.1765
25. Al-Rahbi ZS, Cutajar DL, Metcalfe P, Rosenfeld AB (2018) Dosimetric effects of brass mesh bolus on skin dose and dose at depth for postmastectomy chest wall irradiation. Phys Med 54:84–93. https://doi.org/10.1016/j.ejmp.2018.09.009
26. Alnawaf H, Butson M, Yu PKN (2012) Measurement and effects of MOSkin detectors on skin dose during high energy radiotherapy treatment. Australas Phys Eng Sci Med 35:321–328. https://doi.org/10.1007/s13246-012-0153-1
27. Cuttino LW, Heffernan J, Vera R et al (2011) Association between maximal skin dose and breast brachytherapy outcome: a proposal for more rigorous dosimetric constraints. Int J Radiat Oncol Biol Phys 81:173–177. https://doi.org/10.1016/j.ijrobp.2010.12.023
28. Vargo JA, Verma V, Kim H et al (2014) Extended (5-year) outcomes of accelerated partial breast irradiation using MammoSite balloon brachytherapy: patterns of failure, patient selection, and dosimetric correlates for late toxicity. Int J Radiat Oncol Biol Phys 88:285–291. https://doi.org/10.1016/j.ijrobp.2013.05.039
29. Kirisits C, Rivard MJ, Baltas D et al (2014) Review of clinical brachytherapy uncertainties: analysis guidelines of GEC-ESTRO and the AAPM. Radiother Oncol 110:199–212. https://doi.org/10.1016/j.radonc.2013.11.002
30. Jamalludin Z, Jong WL, Abdul Malik R et al (2019) Characterization of MOSkin detector for in vivo dose verification during cobalt-60 high dose-rate intracavitary brachytherapy. Phys Med. https://doi.org/10.1016/j.ejmp.2019.01.010